# The complex gravitational lens system B1933+503

C. M. Sykes<sup>1</sup>, I. W. A. Browne<sup>1</sup>, N.J. Jackson<sup>1</sup>, D.R. Marlow<sup>1</sup>,

- S. Nair<sup>1</sup>, P. N. Wilkinson<sup>1</sup>, R. D. Blandford<sup>2</sup>, J. Cohen<sup>2</sup>,
- C. D. Fassnacht<sup>2</sup>, D. Hogg<sup>2</sup>, T.J. Pearson<sup>2</sup>, A. C. S. Readhead<sup>2</sup>, D. S. Womble<sup>2</sup>
- S. T. Myers<sup>2,5</sup>, A. G. de Bruyn<sup>4,6</sup>, M. Bremer<sup>3</sup>, G. K. Miley<sup>3</sup> & R. T. Schilizzi<sup>4</sup>
- <sup>1</sup> University of Manchester, NRAL Jodrell Bank, Macclesfield, Cheshire SK11 9DL, England
- <sup>2</sup> California Institute of Technology, Pasadena, CA 91125, USA
- <sup>3</sup> Sterrewacht Leiden, Postbus 9513, 2300RA Leiden, Netherlands
- <sup>4</sup> Joint Institute for VLBI in Europe, Postbus 2, 7990 AA, Dwingeloo, Netherlands
- Dept. of Physics and Astronomy University of Pennsylvania 209 S. 33rd Street Philadelphia, PA 19104, USA
- <sup>6</sup> Kapteyn Laboratory, Postbus 800, 9700 AA Groningen, Netherlands

Oct 17, 1997

#### ABSTRACT

We report the discovery of the most complex arcsec-scale radio gravitational lens system yet known. B1933+503 was found during the course of the CLASS survey and MERLIN and VLA radio maps reveal up to 10 components. Four of these are compact and have flat spectra; the rest are more extended and have steep spectra. The background lensed object appears to consist of a flat spectrum core (quadruply imaged) and two compact "lobes" symmetrically disposed relative to the core. One of the lobes is quadruply imaged while the other is doubly imaged. An HST observation of the system with the WFPC2 shows a galaxy with an axial ratio of 0.5, but none of the images of the background object are detected. A redshift of 0.755 has been measured for the lens galaxy.

**Key words:** instrumentation: gravitation – galaxies: individual B1933+503 – gravitational lensing.

#### 1 INTRODUCTION

The Cosmic Lens All-Sky Survey (CLASS) is a survey of flat-spectrum radio sources whose primary purpose is the discovery of new radio-loud gravitational lens systems. A survey of 10,000 radio sources is being undertaken. Those sources which, when observed with the VLA at 8.4 GHz at a resolution of 200 mas, are found to possess multiple components or very complex structure are followed-up at higher resolution with MERLIN and the VLBA. Higher resolution allows one to separate the genuine lens systems, which consist of multiple flat-spectrum components, from systems containing a flat-spectrum core and steep-spectrum extended radio emission. The discovery of the lenses B1600+434, B1608+656 and B0712+472 has already been announced (Jackson et al. 1995; Myers et al. 1995; Jackson et al. 1997).

In this paper we present VLA, MERLIN and VLBA radio images of B1933+503. We also show a WFPC2 I image of the field together with an optical spectrum obtained with the Keck Telescope. A list of the observations is given in Table 1.

Table 1. Observations of B1933+503

Telescope	Observing date	Exposure time	Frequency or $\lambda$	Resolution (arcsec)
VLA	1994 Mar 2	30 s	8.4 GHz	0.2
MERLIN	1995 Jun 23	$1   \mathrm{hr}$	$5.0~\mathrm{GHz}$	0.04
VLA	1995 July 6	30 min	$15~\mathrm{GHz}$	0.13
VLA	1995 July 6	30 min	$8.4~\mathrm{GHz}$	0.2
VLA	1995 Aug 28	$1   \mathrm{hr}$	$15~\mathrm{GHz}$	0.13
VLA	1995 Sept 2	5 min	$15~\mathrm{GHz}$	0.13
MERLIN	1995 Oct 27	18 hr	$1.7~\mathrm{GHz}$	0.12
Keck	1995 Sept 29	$50 \min$	407 - 911 nm	-
HST	1995 Nov 11	800s	540  nm	0.1
HST	1995 Nov 11	1000s	814 nm	0.1
VLBA	1995 Nov 12	$40 \min$	$5.0~\mathrm{GHz}$	0.0015

#### 2 RADIO AND OPTICAL OBSERVATIONS

The radio maps of B1933+503 are presented in Figure 1. The components are labeled 1 to 8; in addition we identify a weak component (1a) close to 1 (visible in the MERLIN 1.7 GHz map). Component 2 is extended and its morphology suggests that it consists of two merging images (see below). The MERLIN 1.7 GHz map also shows weak emission

between component 2 and component 7. A comparison of the MERLIN  $1.7~\mathrm{GHz}$  map with the MERLIN  $5~\mathrm{GHz}$  map clearly shows that the different components have different spectral behaviours. Note, in particular, components 4 and 5; the latter is one of the brightest components at 1.7 GHz while the former dominates at the higher frequencies. In Table 2 we list the flux densities of the radio components. In Figure 2 we have combined this information to obtain radio spectra for the seven strongest components. We see that 1, 3, 4 and 6 all have flat spectra while the rest are steep. As expected, the flat spectrum components are the most compact. Components 1, 3 and 4 are all detected in the 6 cm VLBA map and all have compact emission on a scale of  $\sim 1$  mas. The other flat spectrum component 6 is also detected, but appears to have a lower surface brightness than components 1, 3 & 4. None of the steep spectrum components are detected.

In order to search for evidence of component variability we have compared the three 15 GHz observations taken at different times. We have used the analysis package DIFMAP (Shepherd et al. 1994) to fit a model consisting of 7 elliptical gaussian components to the data since components 1a and 8 are very weak at 15 GHz. There is some evidence for variability; in particular the flat spectrum components have all changed relative to the steep spectrum components between 1995 July 6 and Aug 28/Sept 2. Since the absolute flux density calibration of the 15 GHz data is not good we have assumed that the steep spectrum emission is not variable and have normalized each epoch to that of Aug 28 in such a way that the sum of the steep spectrum emission is the same on each occasion. In this way we deduce that the flat spectrum components were systematically weaker by between 12% and 33% in July 1995 as compared to Aug/Sept 1995. We take this as tentative evidence for variability.

There is no optical emission from B1933+503 visible on the Palomar Sky Survey. HST observations with WFPC2 were obtained on November 11, 1995 in both V and I bands. The HST observation, with a total exposure time of 1100s in the F814W filter, shows a faint galaxy with a compact core (Figure 3). We believe this to be the lensing galaxy. The integrated I magnitude within an ellipse  $2 \times 1$  arcsec is 20.6±0.2. The galaxy position angle, derived by fitting elliptical isophotes to the light profile, is  $-40\pm5$  degrees. It has a bright compact core with the ellipticity of the low brightness emission increasing to 0.5 outside the central 0.6. In Figure 4 we show a fit to the radial brightness distribution of the I-band (814-nm) HST image. The radial brightness distribution has been obtained by assuming the galaxy to be elliptical with axial ratio 0.5 and collapsing the data on to the major axis. Both disk and de Vaucouleurs models were fitted to the profiles. Overall the de Vaucouleurs profile is the better fit (reduced  $\chi^2 \sim 1$ ) though, if the central 0.2 arcsec is ignored, the disk and de Vaucouleurs models are statistically indistinguishable. The radial profile favours classification as an early-type galaxy, while the ellipticity of 0.5 and the [OII]3727 emission line (see below) are more typical of S0/spiral systems. Clearly data with better sensitivity are needed for a more definitive statement about the nature of the lensing galaxy. The galaxy is not clearly seen in the HST V image, leading to a limit on its integrated V magnitude of about 22.5.

The images of the lensed object are not detected in the HST pictures, down to limiting magnitudes of about 24.2 in I. If the lensed object is a quasar it must therefore be extremely underluminous (especially as it would be expected to be magnified by the lensing), or heavily reddened at optical wavelengths by passage of the light through the lensing galaxy. The only possible point source seen in the image is about 1".4 W, 2".5 N of the lensing galaxy; however, no other images are seen which might correspond to other radio components and we do not have accurate astrometry which would enable us to locate it precisely on the radio map.

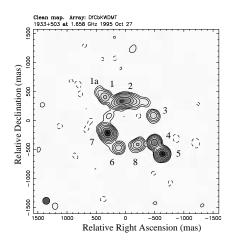
An optical spectrum of B1933+503 was taken with the Keck telescope on Sept 29 1995, using LRIS (Oke et al, 1995). The resulting spectrum is shown in Figure 5. Though the observing conditions were not ideal, one narrow emission line and two absorption lines are detected. We identify the emission line with [OII] at a redshift of 0.755 and the absorption lines with CaII K & H absorption with the same redshift. The galaxy dominates the HST pictures, and hence the emission in the spectrum must be nearly all light from the galaxy, rather than from the images of the background object.

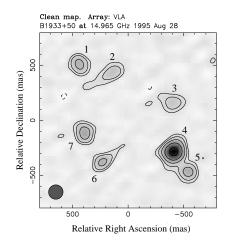
#### 3 B1933+503 AS A LENSED SYSTEM

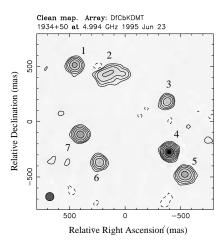
A detailed discussion of a lens model for B1933+503 is given in the companion paper (Nair, 1997). Here we simply discuss the observational constraints in terms of a generic lens model. The large number of features in the radio maps strongly suggests that a multi-component background source is being imaged. We can use the radio spectral information (Figure 2) and the surface brightness information from the radio maps to identify features which could be images of a single background component. It is evident that components 1, 3, 4, and 6 all have very similar peaked spectra and are compact, though we note that the VLBA map indicates that component 6 is somewhat less compact than components 1, 3 and 4. These four components are almost certainly the quadruple images of the core of the background radio source. Components 2, 5 and 7 all have steep spectra down to 1.7 GHz. While the data on components 8 and 1a are less convincing it is likely that they too have steep spectra. The above constraints have been used as a starting point for the model presented by Nair (1997). B1933+503 can be interpreted as the imaging by a single elliptical lens of a compact triple source, consisting of an inverted spectrum core and two steep spectrum "lobes", each separated by  $\sim 70$  mas from the core.

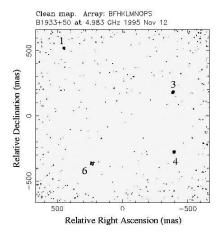
B1933+503 is the first example of a gravitational lens where three compact components are each multiply imaged. As such, it offers the prospect of deriving a quite detailed

Figure 1. Radio images of the B1933+503 system. Top left: MERLIN 1.7-GHz image restored with a  $120 \times 120$  mas. The contours are -1, 1, 2, 4, 8, 16, 32, and 64% of the peak brightness of 0.017 Jy per beam. Top right: VLA 15-GHz image restored with a  $130 \times 130$  mas beam. The contour levels are -4, 4, 8, 16, 32, 64% of the peak brightness of 0.018 Jy per beam. Bottom left: MERLIN 5-GHz image restored with a beam of  $40 \times 40$  mas. The contour levels are -1.5, 1.5, 3, 6, 12, 24, 48, 96% of the peak brightness of 0.019 Jy per beam. Bottom right: VLBA 5 GHz image restored with a beam of  $10 \times 10$  mas. The contour levels are -2, 2, 4, 8, 16, 32 and 64% of the peak brightness of 0.021 Jy per beam.









model of the surface density distribution of the inner parts of the intervening galaxy. Measuring relative time delays between image pairs will contribute to the specificity of this model. However, the failure to detect the lensed images optically and, consequently, the poor prospects for measuring the source redshift, makes us pessimistic that this source will be useful for determining the Hubble constant. More detailed imaging studies with MERLIN and VLBA are underway.

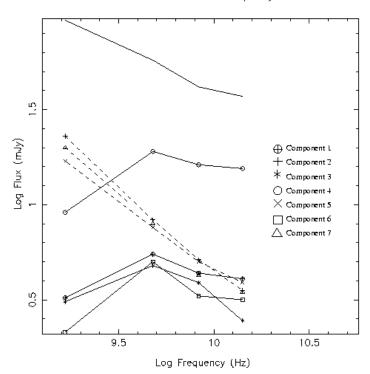
### ACKNOWLEDGMENTS

This research used observations with the Hubble Space Telescope, obtained at the Space Telescope Science Institute, which is operated by Associated Universities for Research in Astronomy Inc. under NASA contract NAS5-26555. The Very Large Array is operated by Associated Universities for Research in Astronomy Inc. on behalf of the National Science Foundation. We thank the W.M. Keck foundation for the generous grant that made the W.M. Keck Observatory possible. MERLIN is operated as a National Facility by NRAL, University of Manchester, on behalf of the UK Particle Physics & Astronomy Research Council. This work was supported in part by the US National Science

## 4 Sykes et al.

Figure 2. Radio spectra for the seven strongest components of B1933+503.





Cpt	Positio	ns (mas)	Flux Density (mJy)			
	RA	DEC	$1.7\mathrm{GHz}$	$5\mathrm{GHz}$	$8.4 \mathrm{GHz}$	$15\mathrm{GHz}$
1	843.5	793.9	3.6	5.6	4.3	4.1
2	519	720	23.0	8.3	4.4	3.5
3	8.0	457.0	2.5	4.7	3.4	2.5
4	0.0	0.0	9.4	19.4	15.7	15.5
5	-134	-198	16.2	7.1	4.5	3.9
6	627	-88	2.2	5.4	3.6	3.2
7	795	165	20.3	8.2	5.2	4.4
8	283	-36	3.6	-	0.5	-
1a	942	883	0.9	-	-	-

**Table 2.** Flux densities of components at various frequencies and their positions measured relative to component 4 (Position (J2000) RA 19 34 30.899, DEC 50 25 23.22). Typical flux density errors are  $\pm 0.4$  mJy. The errors on the relative positions vary; very approximately those for components 1, 3 and 4 which have been obtained from the VLBA 5 GHz data are ≤0.5 mas, for components 5, 6 and 7 from the MERLIN 5 GHz data are ~5 mas and for components 8, 2 and 1a obtained from the MERLIN 1.7 GHz data they are ~20 mas

Foundation under grant AST-9420018 and in part by the European Commission, TMR Programme, Research Network Contract ERBFMRXCT96-0034 "CERES".. CMS and DRM have been supported by PPARC studentships.

Jackson, N., et al., 1997, MNRAS, in press

King, L.J., Browne, I.W.A., Muxlow, T.W.B., Narasimha, D., Patnaik, A.R. Porcas, R.W. & Wilkinson, P.N., 1997, MN-RAS, 289, 450

Myers, S., et al., 1995, ApJ, 447, L5

Nair, S. 1997, Companion paper.

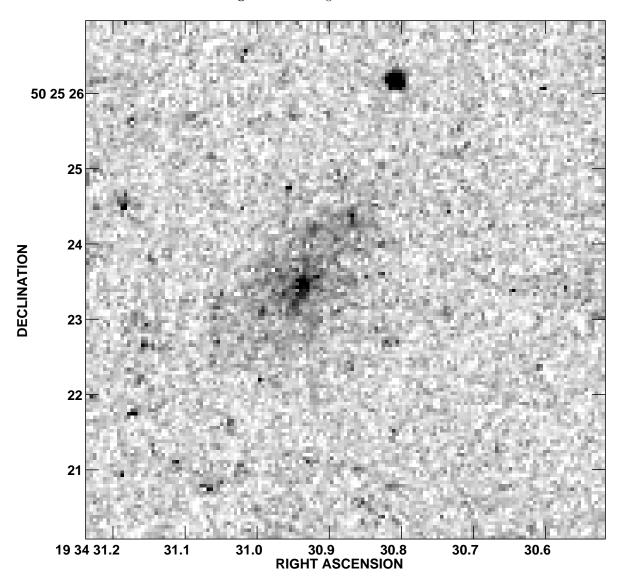
Oke, J.B., Cohen, J.G., Carr, M., Cromer, J., Dingizian, A., Harris, F.H., Labrecque, S., Lucinio, R., Schaal, W. Epps, H. & Miller, J., 1995, PASP, 107, 375.

Shepherd, M.C., Pearson, T.J. & Taylor, G.B. 1994, BASS, 26,

#### REFERENCES

Jackson, N., et al., 1995, MNRAS, 274, L25

Figure 3. HST image taken with F814W filter



## 6 Sykes et al.

Figure 4. Fits to the radial brightness distribution of the I-band (814-nm) HST image. The data points represent the elliptical light distribution collapsed on to the galaxy major axies. Each pixel is gridded to the nearest 10 mas. The counts from any one pixel contribute to just one point. Both disk (exponential) and de Vaucouleurs profiles fits are shown. The latter gives the better fit if the central part of the galaxy is included; a disk profile fits the outer part of the galaxy well. The histogram shows the result of a cut along the major axis.

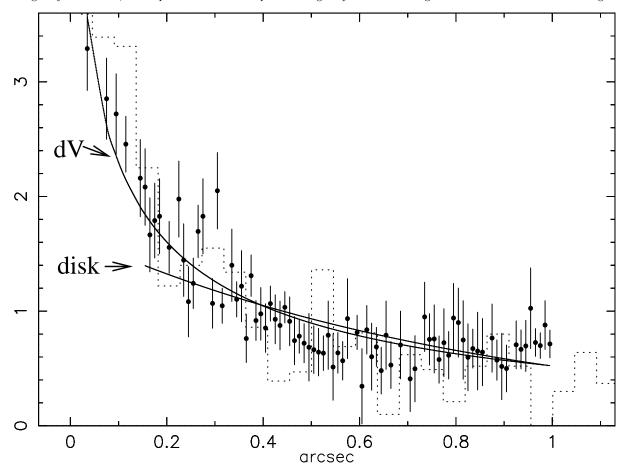


Figure 5. Keck spectrum of 1933+503 taken with LRIS. Only that part of the spectrum between  $6000\text{\AA}$  and 8000Å is displayed. The lower trace shows the rms noise on the spectrum.

